2013 IEEE International Conference on Robotics and Automation (ICRA)
Karlsruhe, Germany, May 6-10, 2013

Gait-Based Compliant Control for Snake Robots

David Rollinson and Howie Choset

Abstract— **We present a method of achieving autonomous compliant behavior in snake robots. This behavior allows snake robots to adapt to changes in its environment, e.g. changes in pipe diameter while climbing. To simplify the task of high-level closed-loop control, the controller uses a low-dimensional gait framework that has been previously used for open-loop trajectory generation. We use an extended Kalman filter (EKF) to estimate the gait parameters that best represent the robot's shape, and then choose a control space of parameters relative to that state. Because this controller specifies whole-body motions of the robot, we are able to generate compliant behavior, even though the joints of the robot contain stiff gear ratios with no mechanical compliance or torque sensing.**

I. Introduction

Snake robots are a class of hyper-redundant mechanisms [1] consisting of kinematically constrained links chained together in series. Their many degrees of freedom allow them to navigate a wide range of environments. To simplify control of our snake robots, cyclic motions (gaits) have been developed that undulate the robot's joints according to parameterized sine waves [2]. These gaits enable an intuitive mapping between changes in a handful of parameters and motion of the robot through the environment. Over the years, our lab has developed gaits that can traverse a variety of terrains, including flat ground and pipes.

Despite having this powerful low-dimensional control framework for commanding motions for our snake robots, closing the loop using this framework has proved to be difficult. To generate motions for the robot, the desired joint angles for each module are determined from the specified gait parameters at each timestep. Each module in the robot contains a low-level controller that drives its joint angle to the commanded angle, and feedback is provided on the module's actual joint angle [3]. We achieve limited compliance with our snake robots by using low proportional gains on our individual modules.

The challenge comes in finding an effective way to incorporate this low-level feedback into our high-level gait-based control. In a sense, we need to find a way in which the low-level errors of individual joints can 'complain' in a meaningful way to a high-level controller built around gait parameters that specify whole-body motions. This work closes the loop by running gait functions in reverse - given a set of joint angles, we fit a parameterized gait function that best describes the shape of the robot. We accomplish this by using an EKF to fit gait parameters to joint angle feedback in real-time.

David Rollinson is a graduate student in the Robotics Institute, Carnegie Mellon University, Pittsburgh, PA, 15213 drollins@cs.cmu.edu
Howie Choset is a professor in the Robotics Institute, Carnegie Mellon University, Pittsburgh, PA, 15213 choset@cs.cmu.edu

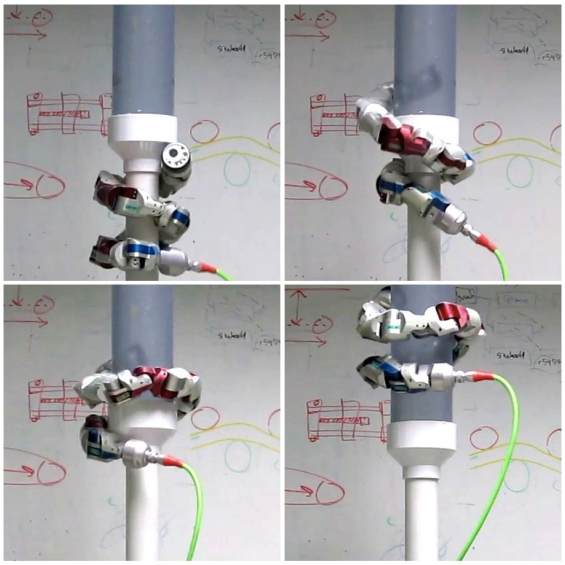

Fig. 1: Montage of the snake robot using gait-based compliant control to autonomously negotiate a transition while climbing up from a 2 inch (5 cm) pipe to 4 inch (10 cm) pipe. This kind of autonomous behavior goes beyond what even a skilled operator can achieve.

Gait-based feedback informs the controller of the state of the robot in a language that it (and the operator) understands, gait parameters. By prescribing simple control laws on gait parameters, we can now create motions that are adaptive to the environmentally constrained state of the robot. Furthermore, these controllers allow us to explore a richer variety of gaits, since a human operator no longer has to be in direct control of each individual gait parameter.

We demonstrate the effectiveness of this control method with motions that are designed for locomoting along pipes. In our experiments, we show that these controllers can extend the capabilities of these gaits beyond what has been previous achieved via remote control. By controlling different gait parameters, the robot is able to climb a pipe that gradually decreases in diameter and safely stop its motion when it meets outside resistance. Notably, this adaptive behavior is compliant enough that it can provide enough force to climb without over-tightening or being unsafe for human contact. The proposed control framework can also execute gaits that have many more parameters than a human operator could control. We use such a gait to reliably climb a pipe that undergoes large changes in diameter (Fig. 1). The proposed compliant controller is also demonstrated in the accompanying video.

978-1-4673-5642-8/13/$31.00 ©2013 IEEE

II. Prior Work

There is a wealth of prior work in motion planning for snake robots. Hirose's pioneering work with the Active Cord Mechanism (ACM) and the formulation of the serpenoid curve [4] laid a foundation for snake robot control that has been pursued in a number of different directions. A survey of a wide variety of gaits, modeling and control strategies for snake robot locomotion is presented in [5].

Overall the methods developed for adaptive behavior in snake robots thus far involve either explicitly changing the snake robot's shape based on feedback from additional sensors on the robot [6] or full knowledge of the robot's pose and the terrain [7], [8]. Even though simple controllers like our lab's parameterized gaits and central pattern generators [9] have had some success, creating autonomous or adaptive behaviors with these controllers has proven difficult.

There is also a long history of exploring compliant control in robotics. Often, it relies on actuators that can perform accurate high-bandwith force or torque control [10]–[12]. Series elasticity actuation has also been proposed as a way of achieving compliance and low-bandwidth force control [13], [14]. Our work achieves compliant control without torque sensing or series elasticity by treating the robot's modules as parallel actuators that contribute to whole body motions.

Our method for gait parameters estimation uses an EKF to efficiently estimate the state of the robot. The EKF is widely used in robotics for system identification and parameter estimation [15], [16]. The state estimator presented here is similar to a formulation presented previously by our group [17].

III. Compliant Control

A. Gaits and Robot Kinematics

To simplify control of the many degrees of freedom used to locomote our robot, we rely on pre-defined undulations that are passed through the length of the robot. Our lab uses parameterized sine waves that are based on Hirose's serpenoid curve [4], and its 3D extensions [18].

Our snake robots consist of a chain of single degree-of-freedom (DOF) modules, where the joints are alternately oriented in the lateral and dorsal planes of the robot [3]. Because of this design, our framework for gaits consists of separate parameterized sine waves that propagate through the lateral and dorsal joints. We refer to this framework as the *compound serpenoid curve*,

$$\theta(n,t) = \begin{cases} \beta_{\text{lat}} + A_{\text{lat}}\sin(\xi_{\text{lat}}) & \text{lateral} \\ \beta_{\text{dor}} + A_{\text{dor}}\sin(\xi_{\text{dor}} + \delta) & \text{dorsal} \end{cases} \tag{1}$$

$$\begin{aligned} \xi_{\text{lat}} &= \omega_{\text{lat}} t + \nu_{\text{lat}} n \\ \xi_{\text{dor}} &= \omega_{\text{dor}} t + \nu_{\text{dor}} n. \end{aligned} \tag{2}$$

In (1) β, A and δ are respectively the angular offset, amplitude, and phase shift between the lateral and dorsal joint waves. In (2) the parameter ω describes the spatial frequency of the macroscopic shape of the robot with respect to module number, n. The temporal component ν determines the frequency of the actuator cycles with respect to time, t.

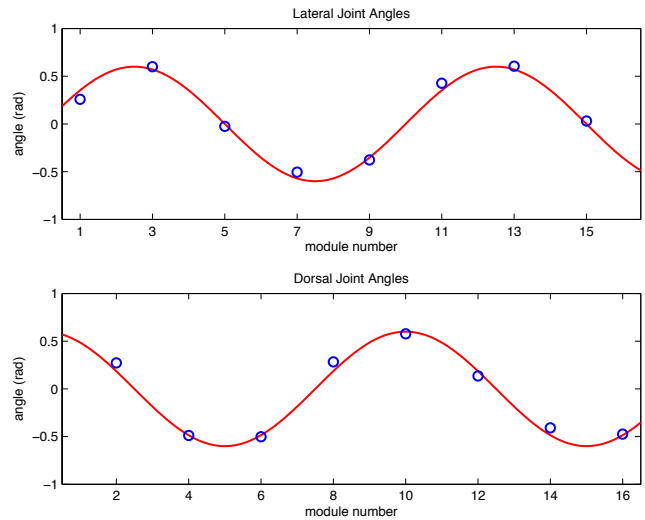

Fig. 2: An example of fitting a parameterized gait to joint angle feedback. The blue circles are actual joint angles from the robot. The red curve is the gait function fit to the robot's joint angles.

The specific gait that we use in this paper is the pole climbing gait, in which the backbone of the robot forms a helix of constant curvature and torsion. To locomote the robot rolls within this shape while squeezing on the outside of a pole. The equation for generating joint angles follows the overall form of the compound serpenoid curve in (1) and (2), but with some of the parameters fixed

$$\bar{\theta}_n = \begin{cases} A{\cdot}\sin(\xi) & \text{lateral} \\ A{\cdot}\sin(\xi + \frac{\pi}{2}) & \text{dorsal} \end{cases} \tag{3}$$

$$\xi = \phi + \nu n. \tag{4}$$

Above, spatial frequency ν and amplitude A are similar to the Frenet-Serret torsion and curvature of the robot's helical backbone shape [20]. The temporal position within the gait controls how the modules are clocked along this backbone, and is controlled by ϕ in (4). To climb the poles of the diameters we used in our experiments (5 cm - 10 cm), ν is set to 0.015.

In a more general sense, the gait equation is just a function that takes in a vector of gait parameters, $\boldsymbol{\alpha}$, and produces a vector of joint angles $\boldsymbol{\theta}$. For the helix gait presented in (3) and (4),

$$\boldsymbol{\alpha} = \begin{bmatrix} \phi \\ A \\ \nu \end{bmatrix}. \tag{5}$$

B. State Estimation

One of the key points of this work is the idea of using the parameters of the gait function to represent the state of the robot. Under typical operation, we command trajectories for the snake robot's modules based on parameterized gait functions similar to (1) and (2). Often, because of limitations of robots actuators or constraints of the environment, the joints of the actual robot do not perfectly execute these

commands. However, by fitting the same parameterized gait functions that we used to generate commands to the feedback joint angles (Fig. 2) we can describe the robot's true shape in the more intuitive and lower-dimensional space of gait parameters.

The EKF uses two functions to iteratively update the robot's estimated state. The first function is the process model that predicts the state at time t, given the previous state at time $t-1$ and the discrete timestep dt. The EKF runs at the same rate as the feedback rate from the robot, approximately 20 Hz.

$$\mathbf{x}_t = f(\mathbf{x}_{t-1}, dt). \tag{6}$$

The process model and measurement model for gait parameter estimation are relatively simple. The state vector of the filter consists of all the gait parameters, $\boldsymbol{\alpha}$, and their first derivatives, $\dot{\boldsymbol{\alpha}}$,

$$\mathbf{x} = \begin{bmatrix} \boldsymbol{\alpha} \\ \dot{\boldsymbol{\alpha}} \end{bmatrix}. \tag{7}$$

At each timestep of the filter, the process model forward integrates the gait parameters based on the current estimated velocity for each parameter. The model assumes a linearly decaying first derivative of the gait parameters

$$\boldsymbol{\alpha}_t = \boldsymbol{\alpha}_{t-1} + \dot{\boldsymbol{\alpha}}_{t-1} \cdot dt \tag{8}$$

$$\dot{\boldsymbol{\alpha}}_t = \lambda \cdot \dot{\boldsymbol{\alpha}}_{t-1}. \tag{9}$$

The decay ratio, λ, was introduced to make the state estimate more stable, especially if the robot experiences a sudden onset of shape change due to outside forces. For the tests in this paper, λ was set to 0.95, but the filter is relatively insensitive to this parameter, and values between 0.50 and 1.00 worked well.

At each prediction step in the filter, the updated covariance of the current state estimate is predicted using to the Jacobian of the process model

$$\mathbf{F} = \frac{\partial f}{\partial \mathbf{x}} \tag{10}$$

and the process noise matrix $\mathbf{Q}$. The process noise is applied to the first derivative of each gait parameter, and reaches the gait parameter via time integration

$$\mathbf{Q} = \int_0^{dt} \mathbf{F}(\tau)\, \boldsymbol{\Psi}\, \mathbf{F}^T(\tau)\, d\tau. \tag{11}$$

In (11), $\boldsymbol{\Psi}$ is a diagonal matrix with the actual noise parameters that get applied to the first derivatives. Carrying out this integration yields

$$\mathbf{Q} = \begin{bmatrix} \psi_1 \frac{dt^3}{3} & 0 & \psi_1 \frac{dt^2}{2} & 0 \\ & \ddots & & \ddots \\ 0 & \psi_n \frac{dt^3}{3} & 0 & \psi_n \frac{dt^2}{3} \\ \psi_1 \frac{dt^2}{2} & 0 & \psi_1 dt & 0 \\ & \ddots & & \ddots \\ 0 & \psi_n \frac{dt^2}{2} & 0 & \psi_n dt \end{bmatrix}. \tag{12}$$

This formulation of process noise reduces the number of tuning parameters for the filter by half, correctly accounts for the amount of time between prediction steps, and adds uncertainty to the appropriate off-diagonals of the covariance matrix [19]. The values for the noise variables ψ_i were tuned by hand and set to between .01 and .001, although changing these parameters by an order of magnitude in either direction did not significantly effect the performance of the EKF.

The second function is the measurement model that predicts sensor measurements for the robot at time t, given the robot's estimated state at time t

$$\mathbf{z}_t = h(\mathbf{x}_t). \tag{13}$$

In the measurement model, joint angles are predicted from the gait equations (3) and (4) using the current timestep's estimated gait parameters, $\boldsymbol{\alpha}$,

$$\bar{\mathbf{z}} = [\, \bar{\theta}_1 \ldots \bar{\theta}_n \,]^T. \tag{14}$$

Each time the filter performs a measurement update, the innovation covariance is calculated using the Jacobian of the measurement model

$$\mathbf{H} = \frac{\partial h}{\partial \mathbf{x}} \tag{15}$$

and the additive measurement noise matrix $\mathbf{R}$.

The measurement noise represents uncertainty in the snake's joint angle encoders and is assumed to be independent and the same magnitude on each joint. This makes $\mathbf{R}$ a diagonal matrix of dimension $n \times n$ where the values on the diagonal are σ

$$\mathbf{R} = \begin{bmatrix} \sigma & \ldots & 0 \\ \vdots & \ddots & \vdots \\ 0 & \ldots & \sigma \end{bmatrix}. \tag{16}$$

The measurement noise parameter σ was set to .0001, based on the approximate uncertainty of our joint angle encoders. However, the filter was fairly insensitive to this parameter.

C. Controller

Once we have an estimated a set of gait parameters, compliant control for the robot is achieved by commanding gait parameter *offsets* from the current estimated state. As the robot is deformed by its environment, the shape changes

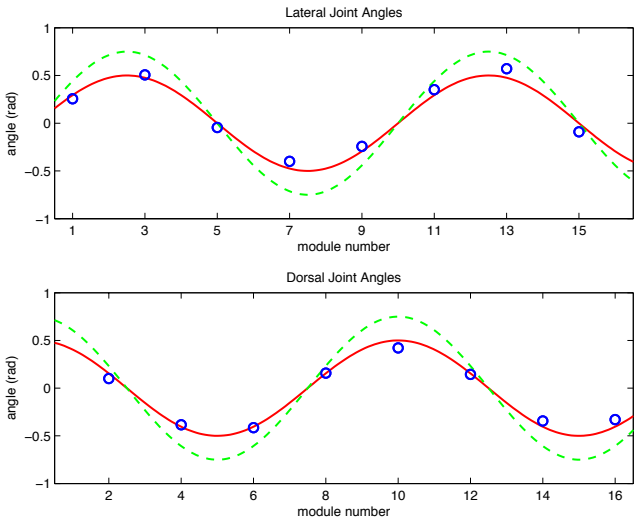

Fig. 3: An example of the commanded function to the snake robot when running the compliant controller on a gait's amplitude. The commanded function (green dashed line) is in phase with the estimated state of the robot, but has a larger amplitude relative the estimated amplitude (red line).

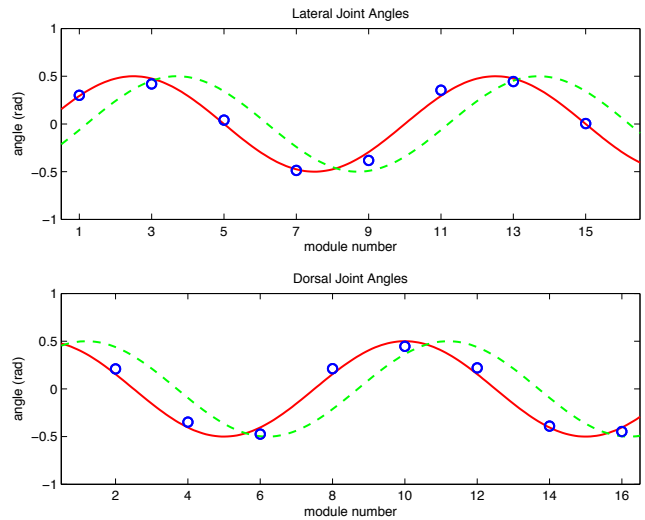

Fig. 4: An example of the commanded function to the snake robot when running the compliant controller on the gait's temporal position. The commanded function (green dashed line) is in phase with the estimated state of the robot, but shifted forward in temporal position.

are represented by the estimated gait parameters and the commanded offsets shift the new commanded gait parameters accordingly. Here we present two examples of compliant control applied to the domain of pipes. Other parameterized gaits can be controlled in similar ways, depending on the desired behavior.

The first controller is 'curvature compliance' where the curvature of the robot is controlled to compliantly squeeze a pipe as its diameter changes. Let $\hat{\boldsymbol{\alpha}}$ be the vector of commanded gait parameters which is normally specified by a human operator

$$\hat{\boldsymbol{\alpha}} = \begin{bmatrix} \hat{\phi} \\ \hat{A} \\ \hat{\nu} \end{bmatrix}. \tag{17}$$

The controller itself is extremely simple. The commanded amplitude, $\hat{A}$, is just a constant offset from the estimated amplitude, A,

$$\hat{A} = A + \rho. \tag{18}$$

If $\rho > 0$, the curvature of the robot will be commanded to be tightened until the environment constrains the shape the robot, and thus results in a controlled 'squeeze' on the pipe. This is intuitively illustrated in Fig. 3. The amount of force the robot exerts on pipe is determined by the value of ρ. Choosing $\rho < 0$ means the curvature of the robot will be commanded to decrease relative to the robot's current curvature. Choosing $\rho = 0$ results in the curvature of the robot's shape complying with whatever outside forces act on it.

The second controller is 'position compliance' where the temporal position of the gait is controlled so that the robot adapts to resistance that it meets progressing forward in the gait cycle. Temporal position modulo 1 can be thought of as the phase within the gait cycle. A positive offset causes the robot to drive forward in the gait cycle, while a negative offset causes it to drive backwards. The larger the offset, the harder the robot tries to push forward. This temporal offset is intuitively illustrated in Fig. 4.

$$\hat{\phi} = \phi + \rho. \tag{19}$$

IV. Experiment

Experiments were run to test compliant control in both amplitude and temporal position. Given good initial parameter estimates, the EKF was observed to be extremely stable and insensitive to the tuning of the process and and measurement noise parameters.

A. Curvature Compliance

Curvature compliance in pole climbing was accomplished by commanding an open-loop velocity in the gait's temporal position while running the compliant controller on the amplitude of the gait's curvature. A compliance offset $\rho = 0.1$ was used. This provided enough squeeze to grip the pole, without straining the modules too hard, and allows vertical climbing on PVC pipes that range in diameter from 5cm to 15cm. Figure 5 shows a montage of the robot making this transition from 10 cm pipe to 5 cm pipe, along with a plot of the gait's estimated and commanded amplitudes over time. As the robot progresses up the pipe, it automatically adapts to the smaller diameter.

B. Position Compliance

Position compliance in pole climbing was accomplished by running the compliant controller on the gait's amplitude and position. The compliance offset for amplitude was the same as the previous experiment. A position compliance offset $\rho = .05$ was used. This value was large enough for the robot to climb against the force of gravity, but small enough that the robot could be stopped by hand. Figure 6 shows a

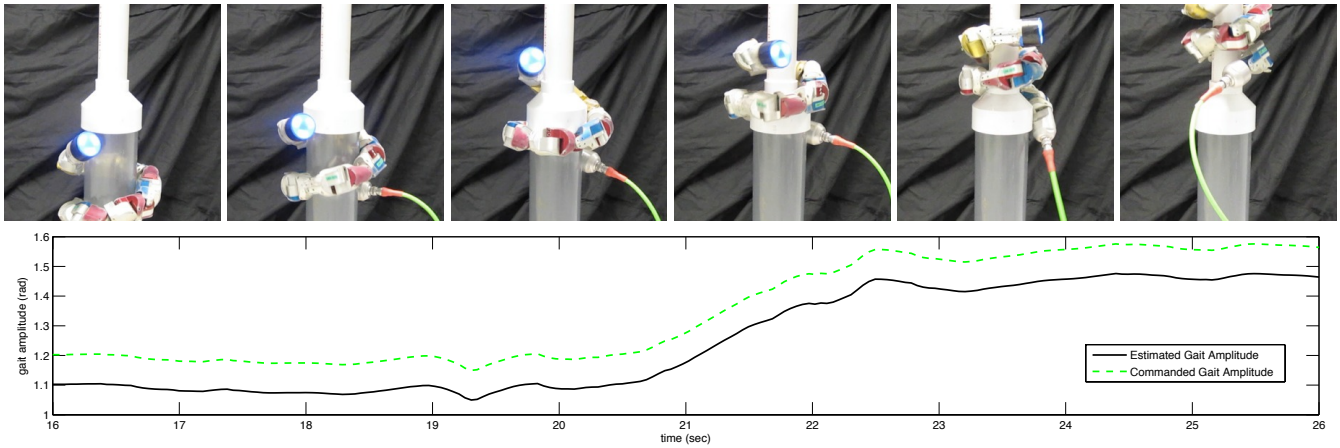

Fig. 5: A montage of the snake robot autonomously transitioning from 4 inch (10 cm) pipe to 2 inch (5 cm) pipe. The green dashed line is the commanded amplitude which is a constant offset of the estimated amplitude of the gait. While the operator could possible have executed this transition by starting the robot off with a significantly tighter curvature, the use of compliant is more energy efficient and handles the transition much more robustly.

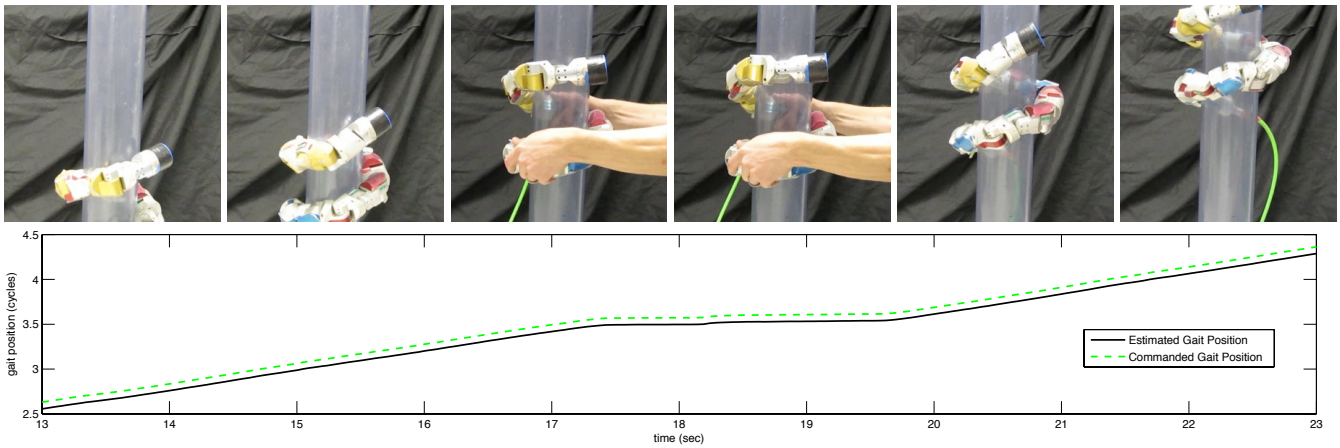

Fig. 6: A montage of the snake robot moving compliantly up a pipe, holding position when held in place, then resuming its motion once released. There is no open-loop motion that can duplicate this behavior. Had the robot been commanded to move forward in temporal position open-loop, it would have eventually broken free of being held, or fallen off the pole entirely.

montage of the robot climbing a 10 cm pipe, along with a plot of the gait's estimated and commanded amplitudes over time.

As the robot progresses up the pipe it is physically held in place for approximately 3 seconds. Rather than blindly push forward, the robot gradually comes to a halt as the controller finds an equilibrium fighting the resistive force of being held. Once the robot is released, it automatically resumes climbing.

V. Conclusions

The proposed gait-based control described here provides an intuitive way to generate high-level behaviors for snake robots. By fitting gait parameters to the feedback joint angles from a snake robot, we are able to describe the state of the robot in terms of the same low-dimensional space as our controls. The EKF allows us to efficiently estimate this gait-based state at each timestep, given the previous state estimate and a set of feedback joint angles.

The controls developed thus far are able to provide compliance particularly well in pipes. This is primarily because of 2 reasons. First, is that the parameters for pipe crawling and pole climbing control whole-body motions that allow the robot's joints to act in parallel, effectively mitigating their stiffness. The second is that because these gaits fully envelop the pipe, the robot can exert more force than it can on flat ground where the robot's contact forces are limited by its own body weight.

We are currently exploring the possibility of adding series elasticity to the joints of the snake robot. This should allow the shape of the robot to be much more sensitive to the terrain it contacts and allow these compliant controllers to work in a wider range of environments. Additionally, sensing the deflection of the elastic element in the joints could allow accurate torque sensing and allow future low-bandwidth force control [13].

The snake robots in our lab contain low-cost gyros and accelerometers in each module. Initial work has already been demonstrated in the estimation of the snake robot's orientation using an EKF to fuse these redundant sensor measurements [17]. An avenue of future research will be

incorporating this estimated orientation into the control of gait parameters. For example, we could put a bend in the robot's shape and using the estimated orientation to keep that bend oriented in some world-frame orientation while crawling through the inside of a pipe. Finally, these methods may be applicable to other systems that have a low-dimensional controller that coordinates a large number of degrees of freedom.

VI. Acknowledgements

The authors would like to Matt Tesch, Florian Enner, and Nate Wood. This work was supported by the DARPA M3 program.

References

[1] G. Chirikjian and J. Burdick, "The kinematics of hyper-redundant robot locomotion," *IEEE Transactions on Robotics and Automation*, vol. 11, no. 6, pp. 781–793, 1995.

[2] M. Tesch, K. Lipkin, I. Brown, R. L. Hatton, A. Peck, J. Rembisz, and H. Choset, "Parameterized and Scripted Gaits for Modular Snake Robots," *Advanced Robotics*, vol. 23, pp. 1131–1158, June 2009.

[3] C. Wright, A. Buchan, B. Brown, J. Geist, M. Schwerin, D. Rollinson, M. Tesch, and H. Choset, "Design and Architecture of the Unified Modular Snake Robot," in *IEEE International Conference on Robotics and Automation (ICRA)*, (St. Paul, USA), pp. 4347–4354, 2012.

[4] S. Hirose, *Biologically Inspired Robots*. Oxford University Press, 1993.

[5] A. A. Transeth, K. Y. Pettersen, and P. l. Liljebäck, "A survey on snake robot modeling and locomotion," *Robotica*, vol. 27, p. 999, Mar. 2009.

[6] P. Liljeback, K. Pettersen, O. Stavdahl, and J. Gravdahl, "Experimental Investigation of Obstacle-Aided Locomotion With a Snake Robot," *Robotics, IEEE Transactions on Robotics*, vol. PP, no. 99, pp. 1–8, 2011.

[7] G. Chirikjian and J. Burdick, "A modal approach to hyper-redundant manipulator kinematics," *IEEE Transactions on Robotics and Automation*, vol. 10, pp. 343–354, June 1994.

[8] J. Burdick, J. Radford, and G. Chirikjian, "A Sidewinding Locomotion Gait for Hyper-Redundant Robots," *Robotics and Automation*, vol. 3, pp. 101–106, 1993.

[9] A. J. Ijspeert, "Central pattern generators for locomotion control in animals and robots: a review.," *Neural Networks*, vol. 21, pp. 642–53, May 2008.

[10] C. Wu and R. Paul, "Manipulator Compliance Based on Joint Torque Control," *IEEE Conference on Decision and Control including the Symposium on Adaptive Processes*, vol. 19, no. 3, pp. 55–71, 1980.

[11] L. Pfeffer, O. Khatib, and J. Hake, "Joint Torque Sensory Feedback in the Control of a PUMA Manipulator," *IEEE Transactions on Robotics and Automation*, vol. 5, no. 4, pp. 418–425, 1989.

[12] D. C. Bentivegna and C. G. Atkeson, "Compliant control of a hydraulic humanoid joint," in *2007 7th IEEE-RAS International Conference on Humanoid Robots*, pp. 483–489, Ieee, Nov. 2007.

[13] G. Pratt and M. Williamson, "Series elastic actuators," *Proceedings 1995 IEEE/RSJ International Conference on Intelligent Robots and Systems.*, pp. 399–406, 1995.

[14] J. Hurst, D. Hobbelen, and A. Rizzi, "Series Elastic Actuation: Potential and Pitfalls," in *International Conference on Climbing and Walking Robots (CLAWAR).*, 2004.

[15] N. Seegmiller, F. Rogers-Marcovitz, and A. Kelly, "Online calibration of vehicle powertrain and pose estimation parameters using integrated dynamics," in *2012 IEEE International Conference on Robotics and Automation*, pp. 3969–3974, Ieee, May 2012.

[16] P. Abbeel, A. Coates, M. Montemerlo, A. Ng, and S. Thrun, "Discriminative training of Kalman filters," in *Robotics: Science and Systems*, 2005.

[17] D. Rollinson, A. Buchan, and H. Choset, "State Estimation for Snake Robots," in *IEEE International Conference on Intelligent Robots and Systems (IROS)*, (San Francisco, USA), pp. 1075—-1080, 2011.

[18] H. Ohno and S. Hirose, "Design of slim slime robot and its gait of locomotion," *Proceedings 2001 IEEE/RSJ International Conference on Intelligent Robots and Systems.*, pp. 707–715, 2001.

[19] P. Zarchan and H. Musoff, *Fundamentals of Kalman Filtering: A Practical Approach*. AIAA (American Institute of Aeronautics & Astronautics), 3rd editio ed., 2009.

[20] H. Yamada and S. Hirose, "Study on the 3D shape of active cord mechanism," in *Robotics and Automation, 2006. ICRA 2006. Proceedings 2006 IEEE International Conference on*, no. May, pp. 2890–2895, IEEE, 2006.